FLOMEKO 2022

A Software Technique for Oil-Water Two-Phase Flow Measurement: CapsNet with Multi-task Learning

L. OuYang, W. K. Ren*, L. D. Bai, N. D. Jin

School of Electrical and Information Engineering, Tianjin University, Tianjin, China
E-mail (corresponding author): renweikai1222@tju.edu.cn

Abstract

Flow parameters measurement is beneficial for understanding oil-water two-phase flow. Due to the changeable flow structures of oil-water two-phase flow, the prediction of superficial velocity of oil-water two-phase flow in large diameter pipes is still a challenging problem. In this paper, a novel soft measurement technique based on Capsule Network (CapsNet) is developed to predict the superficial velocity. Firstly, a vertical upward oil-water two-phase flow experiment in a 125 mm ID pipe was conducted, and response signals at different flow conditions were obtained by a vertical multi-electrode array (VMEA) conductance sensor. Then, in order to increase the number of samples without losing information, a new data pre-processing (1D-to-2D) technique is used. Finally, a novel multi-task learning network based on CapsNet is designed to predict the flow pattern and superficial velocity of each phase. To verify the advancedness of the method, we compared the proposed network with its variations and other competitive networks. The results suggest the proposed network achieves the best performance for prediction of flow pattern and superficial velocity. The proposed method presents great potential for handling high-dimensional, time-varying and nonlinear problems in multiphase flow.

1. Introduction

Oil-water two-phase flow occurs frequently in the petroleum industry [1]. Flow pattern identification is a fundamental issue in two-phase flow study. Also, accurate measurement of flowrate can bring great benefits for well testing, reservoir management, production monitoring. As for the solution of liquid holdup, Maxwell formula [2] assumes that non-contact spherical particles with uniform diameter are randomly distributed in the conductive continuous phase medium. However, the fluid flow process in large pipe diameter is extremely non-uniform distribution, which is different from that in small pipe diameter. The idea of obtaining the phase flowrate by traditional methods is not feasible.

In the early days, the data-driven methods for flow pattern identification were mainly focused on the statistical analysis of the measured signals [3]. Unlike traditional methods, many researchers have regarded machine learning as a potential alternative method for flow pattern prediction [4-6]. Therefore, automatic flow pattern identification for two-phase flows based on machine learning has attracted great research interest. It provides potential solutions for nonlinear systems and generates its own rules for the learned examples. One of the first studies applying machine learning algorithms to two-phase flow pattern recognition was presented by Cai et al [7]. In recent years, deep learning theory has provided a new perspective for the feature representation of complex systems. In contrast to machine learning, deep learning is replacing feature engineering methods. In this method, features are no longer designed by hand, but are learned by back-propagation of trained deep learning models.

By reviewing the survey literature, it is easy to find that there is relatively little research on multi-task learning in flow pattern recognition and superficial velocities prediction [8-12]. For sensor signals, most researchers still perform manual feature extraction. In addition, there is no design and construction of an intelligent recognition depth network to automatically classify these flow patterns by processing multi-channel conductance signals. So, this paper proposes a novel model to solve the problem for non-stationary and non-linear multi-sensor signals of oil-water flow. To the best of our knowledge, the proposed model (sequence-based CapsNet with multi-task learning) is the first attempt to utilize CapsNet for two tasks simultaneously: flow pattern recognition and superficial velocities prediction.

2. Related works

Recently, with human exploration in deep learning, DL methods with more powerful data processing capabilities have been proposed. In this section, related works including the convolution block, residual structure, split-attention block, inception block and capsule network are briefly described.

As shown in Figure 1, the CNNs [13] applies the convolution operation to the incoming multivariate time series, simulating the response of individual neurons to

visual stimuli and passing the results to the next layer. The pooling layer aggregates the output of neuron group of the previous layer into an individual neuron of next layer using pooling operation.

Figure 1: Convolution and pooling operation.

As shown in Figure 2, ResNet [14] adds linear shortcut connections for the convolutional layers, which may potentially enhance the accuracy. The residual structure rationally connects one layer to another by skipping some intermediate layers for specialized information flow across layers.

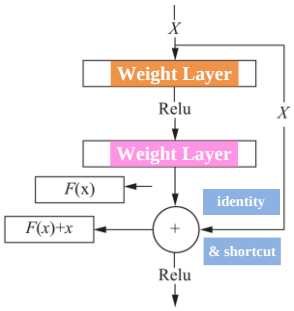

Figure 2: Residual structure.

Attention mechanism [15] guides a model to focus on the most important information in the input, rather than processing the whole input at once. The composition of the ResNeSt is inspired by ResNeXt, SE-Net, and SK-Net. As shown in Figure 3, by introducing split-attention, features with different weights can be obtained between groups of feature maps.

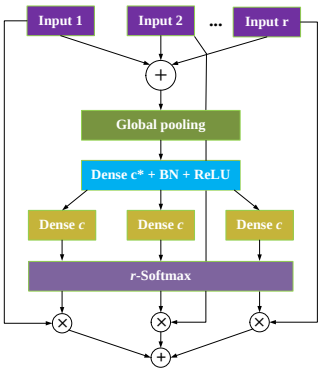

Figure 3: Split-Attention block.

To obtain further deeper feature maps, traditional convolutional neural networks prefer to obtain deeper architectures, which leads to too many parameters that are difficult to train and, more importantly, it increases the consumption of time and space. Inception block provides a different approach to extract deeper feature maps. The architecture of inception block [16] is shown in Figure 4.

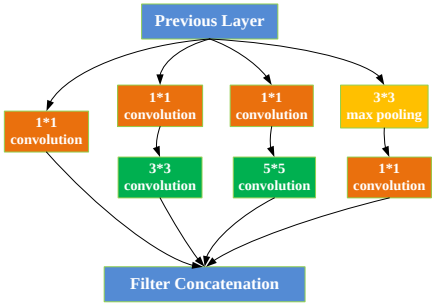

Figure 4: Inception block.

Capsule networks [17] include different hierarchy caps, which can be regarded as layers in traditional neural networks. Its architecture is shown in Figure 5. The capsule network encodes the spatial information and the probability of object existence at the same time, which is encoded in the capsule vector.

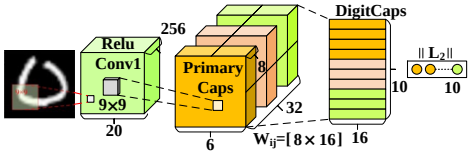

Figure 5: Capsule networks architecture.

In the capsule net, high-level capsules are the weighted sum of the low-level capsules. Dynamic routing [17] is introduced to update the weights. By dynamic routing, the conversion from a low-level capsule to a high-level capsule is complete. The CapsNet uses the similarity of capsules in different layers to update the weights, that is, the dynamic routing algorithm, as shown in Figure 6.

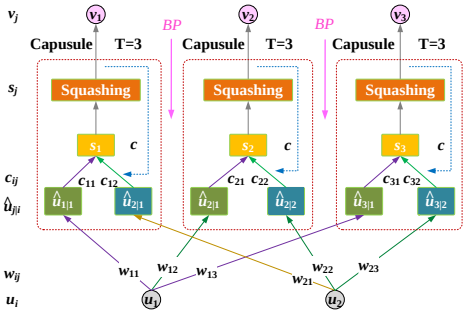

Figure 6: Dynamic routing algorithm.

3. Proposed method

First, the input is pre-processed and then, is fed to the model for the task completion. The whole architecture is shown in Figure 7.

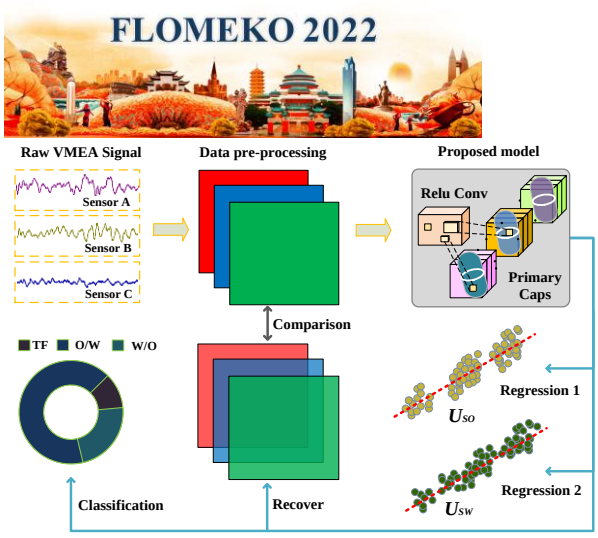

Figure 7: The complete proposed proposal for multi-task learning.

3.1 Pre-processing of raw sensors data

Considering that the input to the CapsNet is two-dimensional, as shown in Figure 8, the raw sensor data also needs to be changed from one dimension to two dimension (1D-to-2D) in the pre-processing. Finally, normalization of the data is also required for better training of the network.

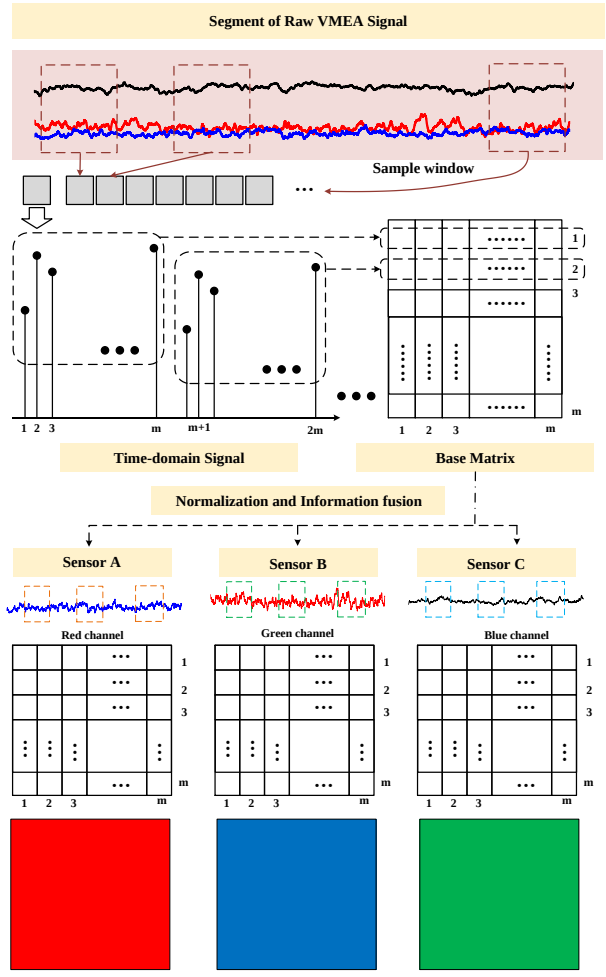

Figure 8: Sensors signal 1D-to-2D conversion method.

3.2 Model architecture

The structure of the proposed model is shown in Figure 9. CapsNet mainly includes multi-set attention layer, residual layer, inception layer, part-connected primaryCaps layer, digitCaps layer and outputCaps layer.

First, the dimension is improved with convolution blocks (1*1 convolution kernel) on the two-dimensional input data, and the focused features are extracted using a multi-set attention block, and then the dimension is recovered with convolution blocks (1*1 convolutional kernel). Then, the new features and the original data (both of the same size) are stacked by the residual structure to obtain the augmented data. Immediately after, the augmented data is extracted with multi-scale features using an inception block. Finally, the constructed vector group neurons pass the multi-scale features to the digital capsule layer for multi-task through an improved dynamic routing.

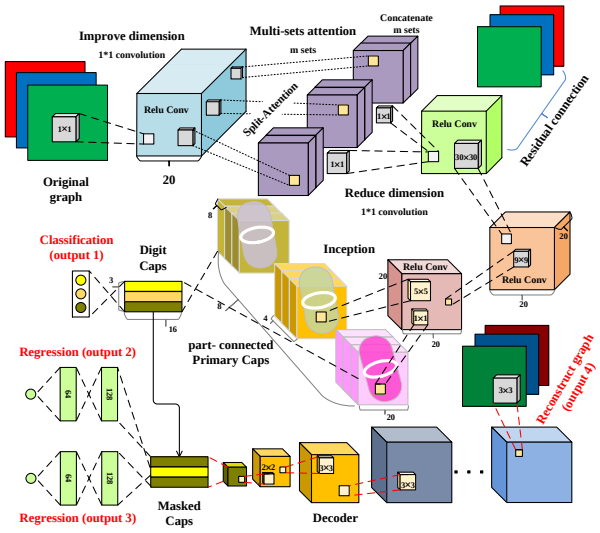

Figure 9: Architecture of proposed model.

4. Data acquisition experiment

As shown in Figure 10, the conductance probe array consists of five stainless steel probes A, B, C, D and E, which are inserted into the pipe at a depth of 1/8D, 1/8D, 1/4D, 1/4D and 1/2D (D is the pipe diameter), and the axial distance between the probes is 15 cm. The probe is powered by 5V DC power supply, when the needle electrode is in contact with non-conductive oil phase, the measurement circuit is off and high voltage is output; while when the needle electrode is in contact with the conductive water phase, the output is low voltage.

The ring conductance measurement system is based on the Vertical Multi-Electrode Array (VMEA) conductance sensor developed in our laboratory [18]. The VMEA consists of a pair of excitation electrodes

E1-E2, one sensor (sensor C) for global measurements of the flow structure and two sensors (sensor A and sensor B) for local measurements. A sinusoidal 20 kHz excitation source with an effective voltage of 1.4 V is used for excitation.

The oil-water two-phase flow dynamics experiments were conducted in a multiphase flow loop apparatus at Tianjin University, as shown in Figure 10. It mainly consists of three parts: oil-water two-channel supply system, flow loop pipeline and control system. In the experiment, the internal diameter (ID) of the pipeline is 125 mm, the oil phase is No. 15 industrial white oil (density: 845 kg/m^3, viscosity: 11.984 mPa·s), and the water phase is tap water (density: 1000 kg/m^3, viscosity: 1 mPa·s).

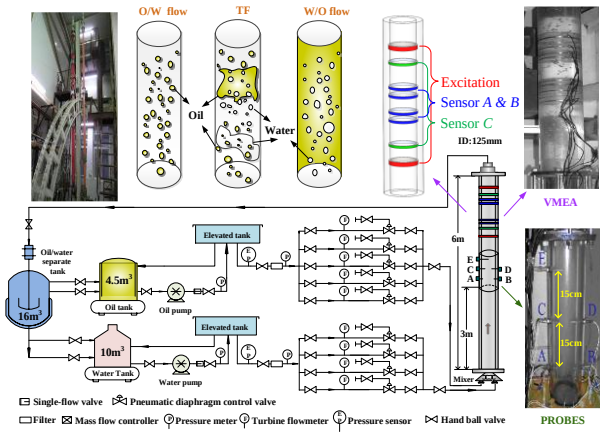

Figure 10: Oil-water Flow Loop Facility.

The experimental design was to first fix the water phase flow velocity with a peristaltic pump, and then gradually increase the oil phase flow velocity. When the oil and water phases are fully mixed in each flow condition, the oil-water phase flow patterns are observed by visual observation, and the output signal of the measurement system is recorded. The range of water flowrate Q_w in this experiment is 0.21 m^3/h - 7.5 m^3/h and the range of oil flowrate Q_o is 0.21 m^3/h - 15.2 m^3/h.

Throughout the experiment, we also observed three typical flow patterns, as shown in Figure 10. For oil-in-water flow (O/W), the dispersed phase is the oil phase, and most of the small oil bubbles are dispersed in the water flow and slowly rise with the fluid. For transitional flow (TF), a large number of oil bubbles gather into oil blocks, while a large number of water bubbles gather together to form water blocks, and the oil and water blocks rise and roll up and down with the fluid at the same time, which is an unstable flow state. For water-in-oil flow (W/O), many small water droplets are densely dispersed in the oil flow.
As shown in Figure 11, during the experiment, a total of 99 experimental results were obtained at different oil/water phase superficial velocity ratio settings.

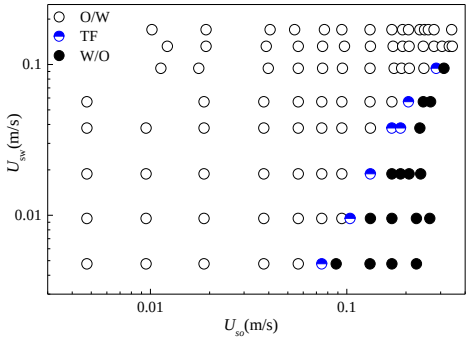

Figure 11: Experimental flow map at different oil/water phase superficial velocities.

Several highly differentiated flow patterns during oil-water flow were indeed found to exist, and they can be more clearly identified by high-speed photography. However, the large differences observed in the flow pattern maps are not the focus of this research paper, which aims at the intelligent identification of the sensor output signals. On the other hand, the flowrate parameters are obtained by combining the known cross-sectional area of pipe and the predicted superficial velocity of each phase.

As shown in Figure 12, for the oil-in-water flow (O/W), the conductance fluctuation signal bounces up and down arbitrarily with randomness; for the transitional flow (TF), the conductance fluctuation signal bounces up and down with pseudo-periodic characteristics; for the water-in-oil flow (W/O), the conductance fluctuation signal is a random noise signal, limited by the properties of the VMEA measurement system.

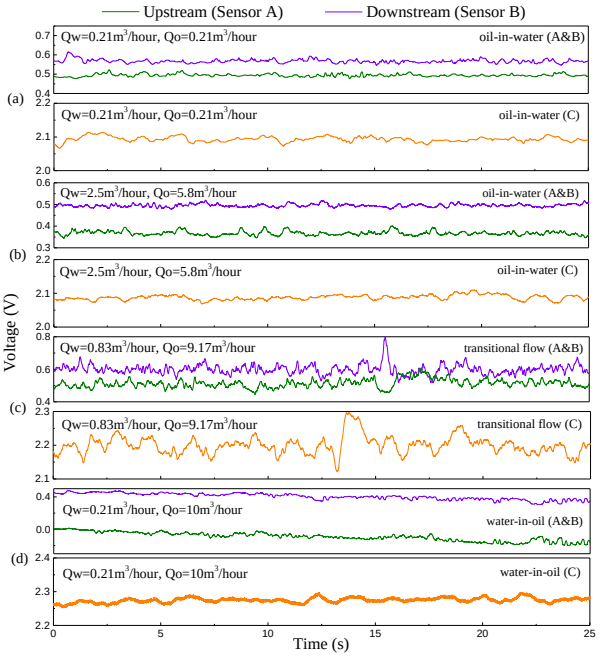

Figure 12: The signals of VMEA for three typical flow patterns: (a) O/W flow: Q_w = 0.21 m^3/h, Q_o= 0.21 m^3/h; (b) O/W flow: Q_w = 2.5 m^3/h, Q_o = 5.8 m^3/h; (c) TF: Q_w = 0.83 m^3/h, Q_o = 9.17 m^3/h. (e) W/O flow: Q_w = 0.21 m^3/h, Q_o = 10 m^3/h.

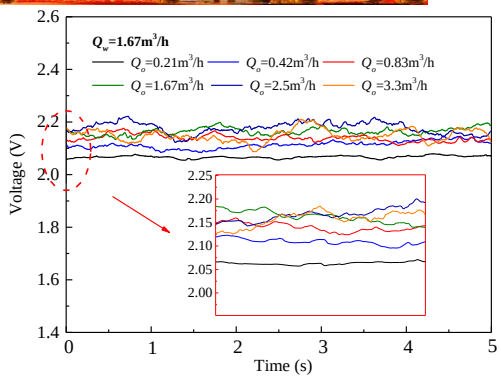

Figure 13: The output signal of VMEA under different flow conditions with constant water phase flowrate (Q_w=1.67 m³/h).

4. Software measurement implementation

As shown in Figure 13, it can be seen from the signal analysis that for the O/W flow, the signal fluctuates between 2.0 V and 2.2 V. Since the fluctuating fundamental value of the conductance signal in the O/W flow varies too slightly, and thus the water holdup cannot be obtained through the Maxwell formula.

In the experimental evaluation, various evaluation criteria are chosen to verify the effectiveness and correctness of the models. ACC is the ratio of the number of correctly predicted samples to the total number of samples. To visually evaluate the prediction results, here we introduce three commonly used regression analysis indexes, namely mean absolute error (MAE) and mean absolute percentage error (MAPE), symmetric mean absolute percentage error (SMAPE).

$$\mathrm{MAE} = \frac{1}{m}\sum_{i=1}^{m}|\hat{y}_i - y_i| \quad (1)$$

$$\mathrm{MAPE} = \frac{100\%}{m}\sum_{i=1}^{m}\left|\frac{\hat{y}_i - y_i}{y_i}\right| \quad (2)$$

$$\mathrm{SMAPE} = \frac{100\%}{m}\sum_{i=1}^{m}\frac{|\hat{y}_i - y_i|}{(|\hat{y}_i| + |y_i|)/2} \quad (3)$$

In this paper, a series of comparative experiments are completed on TensorFlow, Google's open deep learning platform. The architecture is based on TensorFlow to implement network training and testing, and is completed on a workstation with Intel(R) i7-6950X CPU and NVIDIA RTX 2080Ti GPU (11 GB graphic memory) and 32 GB memory.

The sample is randomly divided into training set, validation set and test set at a ratio of 7:2:1. The raw signals after pre-processing were used for model training process. In the experiments, we fixed some parameters based on experience. Adam and backpropagation are taken to optimize. The initial learning rate is 0.01, and it decays by half every 5 epochs. Moreover, the batch size is 32 and the number of epochs is 50. The dimension of the category capsule is set to 3. Run 5 times to average the results. Set all the above parameters to obtain satisfactory classification accuracy and keep it constant in oil-water flow dataset.

5. Experimental study

Figure 14 gives the performance of the proposed model on the test set with respect to the estimation of the superficial velocities of both phases. It can be noticed that the model also has a good estimation capability on the test set.

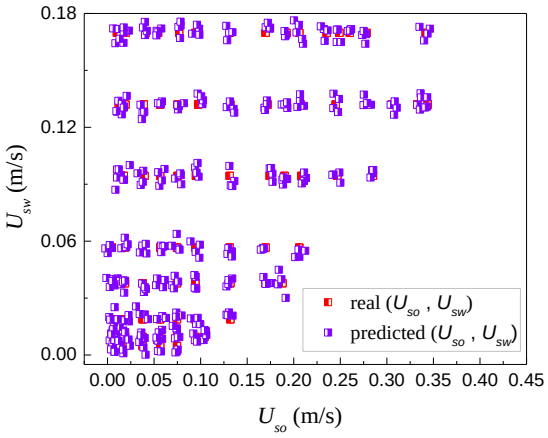

Figure 14: The prediction results of the combination (U_{so}, U_{sw}) based on our trained model on test set.

It should be emphasized that this part of the experiment is based on a complete churning of the data, where each flow condition data is distributed and present in the training set, validation set and test set. Slicing each type of data with different steps of sliding windows ensures a balanced and sufficient amount of data for each type. To objectively test the performance of the proposed model, it was compared with other models that have proven to be very effective in the field of parametric prediction.

Table 1: Comparative tests on ACC and SMAPE of different models.

Model	SVM [19]	DNNs [21]	Cap [24]	Proposed
ACC	0.9212	0.9605	0.9915	0.9984
Model	SVR [20]	LSTM [22]	CNTM [23]	Proposed
SMAPE	9. 20%	6. 97%	4.64%	1.53%

6. Conclusion

These interesting and meaningful findings suggest that CapsNet can reveal nonlinear time series containing extreme details of the flow structure, and furthermore, the model proposed is highly capable of dealing with high-dimensional, time-varying and nonlinear problem, and has great potential for complex measurement systems.

Acknowledgments

This study was supported by National Natural Science Foundation of China (Grant No. 42074142, 51527805).

References

[1] Izwan Ismail A. S., Ismail I., Zoveidavianpoor M., Mohsin R., Piroozian A., Misnan M. S., Sariman M. Z., "Review of oil-water through pipes", *Flow Measurement and Instrumentation*, **45**, 357-374, 2015.

[2] Maxwell J. C., "A treatise on electricity and magnetism", *Nature*, **7**, 478-480, 1873.

[3] Ding H., Huang Z. Y., Song Z. H., Yan Y., "Hilbert-Huang transform based signal analysis for the characterization of gas-liquid two-phase flow", *Flow Measurement and Instrumentation*, **18**, 37-46, 2007.

[4] Mi Y., Ishii M., Tsoukalas L. H., "Vertical two-phase flow identification using advanced instrumentation and neural networks", *Nuclear Engineering and Design*, **184**, 409-420, 1998.

[5] Hernández L., Juliá J. E., Chiva S., Paranjape S., Ishii M., "Fast classification of two-phase flow regimes based on conductivity signals and artificial neural networks", *Measurement Science and Technology*, **17**, 1511, 2006.

[6] Rosa E. S., Salgado R. M., Ohishi T., Mastelari N., "Performance comparison of artificial neural networks and expert systems applied to flow pattern identification in vertical ascendant gas-liquid flows", *International Journal of Multiphase Flow*, **36**, 738-754, 2010.

[7] Cai S., Toral H., Qiu J., Archer J. S., "Neural network based objective flow regime identification in air-water two phase flow", *Canadian Journal of Chemical Engineering*, **72**, 440-445, 1994.

[8] Al-Wahaibi T., Mjalli F. S., "Prediction of horizontal oil-water flow pressure gradient using artificial intelligence techniques", *Chemical Engineering Communications*, **201**, 209-224, 2014.

[9] Azizi S., Awad M. M., Ahmadloo E., "Prediction of water holdup in vertical and inclined oil-water two-phase flow using artificial neural network", *International Journal of Multiphase Flow*, **80**, 181-187, 2016.

[10] Amar N., Menad N. Z., Redouane K., "Bottom hole pressure estimation using hybridization neural networks and grey wolves optimization", *Petroleum*, **4**, 419-429, 2018.

[11] Wang H. K., Zhang M. M., Yang Y. J., "Machine learning for multiphase flowrate estimation with time series sensing data", *Measurement: Sensors*, **10-12**, 100025, 2020.

[12] Wang H. K., Hu D. L., Zhang M. M., Yang Y. J., "Multiphase flowrate measurement with time series sensing data and sequential model", in *IEEE International Instrumentation and Measurement Technology Conference (I2MTC)*, 1-6, 2021.

[13] Du M., Yin H. Y., Chen X. Y., Wang X. Q., "Oil-in-water two-phase flow pattern identification from experimental snapshots using convolutional neural network", *IEEE Access*, **7**, 6219-6225, 2019.

[14] He K. M., Zhang X. Y., Ren S. Q., Sun J., "Deep residual learning for image recognition", in *IEEE Conference on Computer Vision and Pattern Recognition (CVPR)*, 770-778, 2016.

[15] Zhang H., Wu C. R., Zhang Z. Y., Zhu Y., Lin H. B., Zhang Z., Sun Y., He T., Mueller J., Manmatha R., Li M., Smola A., "ResNeSt: Split-Attention Networks", arXiv preprint arXiv:2004.08955, 2020.

[16] Szegedy C., Liu W., Jia Y., Sermanet P., Reed S., Anguelov D., Erhan D., Vanhoucke V., Rabinovich A., "Going deeper with convolutions", in *IEEE Conference on Computer Vision and Pattern Recognition (CVPR)*, 1-9, 2015.

[17] Sabour S., Frosst N., Hinton G. E., "Dynamic routing between capsules", in *31st Conference on Neural Information Processing Systems (NIPS)*, 3859-3869, 2017.

[18] Jin N. D., Zhao X., Wang J., Wang Z. Y., Jia X. H., Chen W. P., "Design and geometry optimization of a conductive probe with a vertical multiple electrode array for measuring volume fraction and axial velocity of two-phase flow", *Measurement Science and Technology*, **19**, 045403, 2008.

[19] Hanus R., Zych M., Kusy M., Jaszczur M., Petryka L., "Identification of liquid-gas flow regime in a pipeline using gamma-ray absorption technique and computational intelligence methods", *Flow Measurement and Instrumentation*, **60**, 17-23, 2018.

[20] Gandhi A. B., Joshi J. B., Kulkarni A. A., Jayaraman V. K., Kulkarni B. D., "SVR-based prediction of point gas hold-up for bubble column reactor through recurrence quantification analysis of LDA time-series", *International Journal of Multiphase Flow*, **34**, 1099-1107, 2008.

[21] Nnabuife S. G., Kuang B., Whidborne J. F., Rana Z., "Non-intrusive classification of gas-liquid flow regimes in an S-shaped pipeline riser using a Doppler ultrasonic sensor and deep neural networks", *Chemical Engineering Journal*, **403**, 126401, 2021.

[22] Zhang Y. C., Azman A. N., Xu K. W., Kang C., Kim H. B., "Two-phase flow regime identification based on the liquid-phase velocity information and machine learning", *Experiment in Fluids*, **61**, 212, 2020.

[23] Dang W. D., Gao Z. K., Hou L. H., Lv D. M., Qiu S. M., Chen G. R., "A novel deep learning framework for industrial multiphase flow characterization", *IEEE Transactions on Industrial Informatics*, **15**, 5954-5962, 2019.

[24] Ren H., Lu H., "Compositional coding capsule network with k-means routing for text classification", *Pattern Recognition Letters*, **160**, 1-8, 2022.